



**"Gheorghe Asachi" Technical University of Iasi, Romania**



---

## **PERMEABILITY MUTATION MECHANISM OF HYDRO-GEOCHEMICAL CONDITIONS IN SEA AND FRESHWATER TRANSITIONAL ZONE**

**Jiaguo Ren<sup>1</sup>, Qianqian Wu<sup>1\*</sup>, Puchuang Gao<sup>1</sup>, Xing Wang<sup>1</sup>, Ke Gong<sup>1</sup>,  
Dongsheng Wang<sup>2</sup>, Tongqian Jia<sup>1</sup>, Xixi Ren<sup>1</sup>**

<sup>1</sup>*College of Earth Science and Engineering, Shandong University of Science and Technology, Qingdao 266590, China*

<sup>2</sup>*Ocean University of China, Qingdao 266100, China*

---

### **Abstract**

Taking the sandy aquifer intruded by seawater in the lower reaches of Dagu River as the research object, the samples of underground freshwater, seawater and aquifer media were collected, and their composition and properties were determined. The seepage device was used to simulate the displacement process of seawater and freshwater. The relationship between permeability change of aquifer and hydrologic-geochemical action was studied. The mechanism of water sensitivity was explained by a hydrologic-geochemical process for the first time. The results show that the exchange and migration of multi-component ions occur in the process of mutual displacement of saline and freshwater, accompanied by clay release and complex hydrologic-geochemical processes. The reason for clay release is not the enhancement of diffusion and dispersion, but the enhancement of clay expansion and diffusion by hydrologic-geochemical action, which results in the decrease of permeability of the aquifer.

**Key words:** hydrologic-geochemistry, permeability, sea and freshwater displacement, water sensitivity

*Received: October, 2019; Revised final: March, 2020; Accepted: April, 2020; Published in final edited form: September, 2020*

---

### **1. Introduction**

Salt-freshwater transitional zone refers to the transitional zone of salt concentration formed by hydrodynamic dispersion between saltwater and freshwater in underground aquifers, which is a transitional zone from high salinity saltwater to low mineralized groundwater. Under offshore hydrogeological conditions, due to natural changes and human factors, the salt-freshwater transitional zone must oscillate back and forth (saltwater-freshwater displacement each other), accompanied by permeability changes of aquifer media and complex hydrologic-geochemical processes (Appelo and Willemsen, 1987; Beekman et al., 1990; Ochi and Vernoux, 1998; Sen and Khilar, 2006).

Water sensitivity refers to the phenomenon of clay release, migration and deposition caused by incompatible external fluids entering porous media, which leads to the decrease of permeability of water-bearing media. Since Fancher first discovered the phenomenon of water sensitivity in 1933, Chinese and researchers and outside China have studied the development of oil and gas reservoirs, soil permeability and groundwater pollution (Chītimuş et al., 2014; Falade et al., 2019; Kafisanwo et al., 2018; Liu et al., 2014; Mawarni et al., 2018; Ren et al., 2018; Wu et al., 2015; Xu et al., 2018; Zhang et al., 2016). However, little research has been done on the changes of the permeability of the sea and freshwater interface, and the effects of hydrologic-geochemistry on the characteristics of aquifer media and aquifers (Du et al.,

---

\* Author to whom all correspondence should be addressed: e-mail: renjiagu008@126.com; Phone: +86 15966929600

2017; Kong et al., 2015; Wu et al., 2018). The effect of permeability has not been reported yet.

In this paper, the behavior of hydrogeochemical processes such as multi-component ion exchange under the influence of water sensitivity in the salt-freshwater transitional zone is studied. The displacement process is simulated by using a displacement device, while the permeability change of aquifer medium as well as the change law of main ions are measured during the displacement process. The dynamic parameters of the aquifer medium and water are attempted to study (Han et al., 2017; Yu et al., 2014; Wang and Shi, 2019). From hydrodynamics and geochemistry perspective, the phenomenon of water sensitivity is explained, which provides a more reasonable scientific basis for the phenomenon that clay release leads to the decrease of aquifer permeability in the process of displacement.

## 2. Test materials and methods

### 2.1. Test materials

The main water samples used in the experiment are groundwater, Dagu River water and seawater collected. Groundwater is taken from Dongxiaobu Village, far from the Dagu River estuary, and seawater is taken from Xiaoqingdao, near Jiaozhou Bay. The water is sealed and preserved, and filtered with 0.45  $\mu\text{m}$  microporous membrane before the test to remove impurities. The water quality analysis results are shown in Table 1.

The test sand samples are undisturbed soils collected from Maoxi Village in the lower reaches of the Dagu River. The bulk density, water content and specific gravity of the sand samples are 1.6 g  $\text{cm}^{-3}$ , 22.10% and 2.65, respectively. The sand samples are air-dried, crushed and sifted, and the grain size of the sand samples is analyzed. For sand samples with particle size larger than 0.075 mm, the screening method is used, while for particles with particle size smaller than 0.075 mm, the hydrometer method is used to determine. According to the results of particle size analysis, the fraction with particle size less than 0.5 mm accounted for 60.52% of the total, the fraction with particle size less than 0.075 mm accounted for 20.42% of the total, and the clay with particle size less than 0.005 mm accounted for only 2.99%. The non-uniformity coefficient of sand sample is 4.45 and the average particle size is 0.397.

The mineral composition of aquifer samples is determined by X-ray diffraction analysis. Firstly, the samples were manually ground into powder. Then, the samples were measured by the Japanese D/maxrB Anode Rotating X-ray Diffractometer under the condition of monochrome radiation. The data were analyzed by JIFFRAC XRD commander software. According to the results of X-ray diffraction analysis, the sand samples are mainly composed of quartz and potassium feldspar, of which 27% are quartz, 67%

potassium feldspar, and only 1.7% are clay minerals.

### 2.2. Test device

The saltwater displacement test adopts a fixed head water flow system, which consists of a fixed head device, a seepage column and an outflow measurement system. The experimental device is shown in Fig.1. The soil column consists of a plexiglass column with a sampling inlet and a water inlet. To eliminate the effect of gravity on particle migration, the seepage column is placed horizontally.

The fixed head device is a vessel with intake, a catchment and a water injection port. The catchment port plays a role of a fixed water level, i.e. adjusting the position of the upper end of the water injection port, so that surplus water or solution can flow out from the catchment port, and always ensure that a small amount of water flows out slowly, so that the water level in the bottle is constant. Besides, the buffer bottle itself has a certain volume.

Once the catchment is faulty or the water supply is insufficient, the water or solution in the buffer bottle will play a buffer role, which will not change the seepage condition of the seepage column dramatically, leading to the failure of the test. It should be noted that when converting the water solution, the intake head and the outlet head should be kept unchanged.

### 2.3. Test method

- (1) The equal bulk density (1.6 g/ $\text{cm}^3$ ) of the aquifer sand sample is loaded into the organic glass tube with a length of 20 cm and an inner diameter of 2.8 cm. Vacuum for 20 minutes with Auto-science vacuum filter under sealed condition and then seawater saturated sand column.

- (2) Connect the saturated sand column with the fixed head system and enter the sea-water at a given hydraulic gradient until the volume of the effluent from the sand column reaches a stable value.

- (3) Directing the three-way valve to river water, the salt concentration of sand column infiltration solution is reduced instantaneously, and the volume, conductivity and absorbance of sand column effluent at different time intervals are measured.

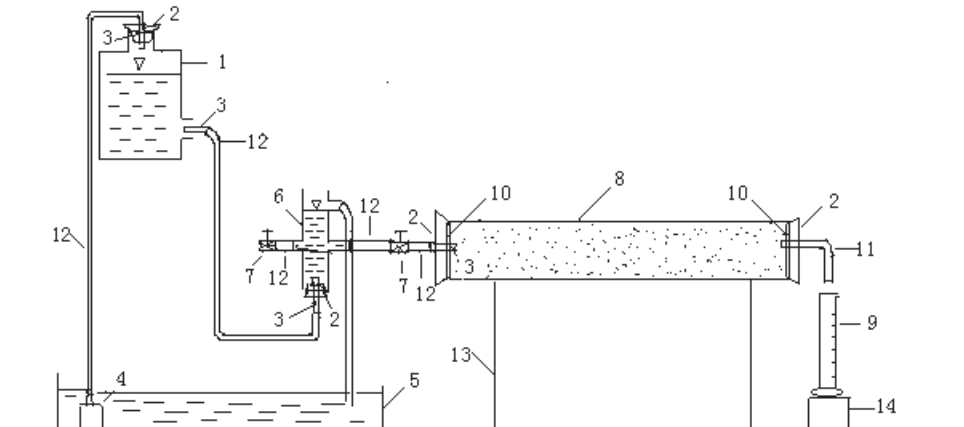
- (4) The volume, conductivity and absorbance of effluent from the sand column at different time intervals were continuously measured by changing the three-way valves according to the sequence of seawater - river water - seawater - river water - seawater - river water.

- (5) According to the volume of the effluent, the flow rate of the effluent can be calculated, and the concentration of suspended particles in the effluent can be determined by the standard curve of absorbance and particle concentration. In this way, the curves of different effluent concentrations with time can be drawn.

**Table 1.** Results of chemical compositions in water samples

Items	$Na^+$	$K^+$	$Ca^{2+}$	$Mg^{2+}$	$Cl^-$	$SO_4^{2-}$	$HCO_3^-$	EC	pH
Seawater	10207.24	340.09	411.30	1282.98	17686.09	2363.55	130.00	48500	8.18
Groundwater	95.95	10.12	151.93	32.07	79.82	141.54	376.13	6315	7.75
River water	5.9	1.3	1.0	1.4	4.1	0.8	1.6	780	7.12

Note: ion concentration in mg/L and conductivity (EC) in  $\mu\text{s}/\text{cm}$

**Fig. 1.** Schematic diagram of the experimental setup

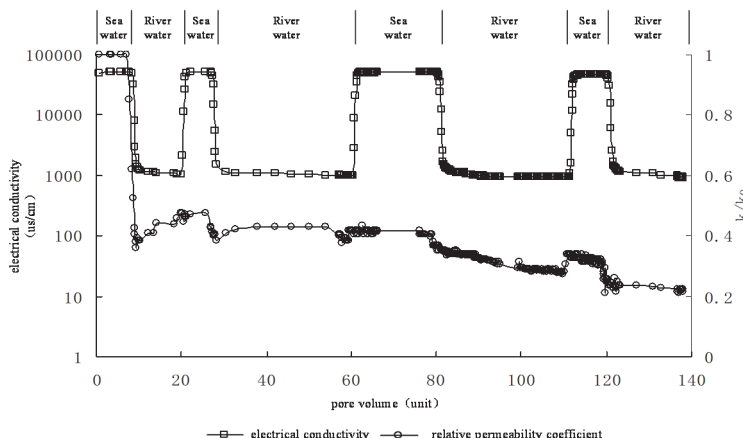
1. Marriotte bottle; 2. Plug; 3. Glass tubing; 4. Pump; 5. Water tank; 6. Constant head tube; 7. Flatjaw pinchcock; 8. Seepage column, 100cm length, 4.3cm inner diameter; 9. Measuring cylinder; 10. Boulting cloth; 11. Glass pipe bending; 12. Rubber pipe; 13. Holder; 14. Plate

### 3. Analysis of permeability mutation test results

Test results show that the solution to the salt concentration changes of permeability changes, especially in the river water, sand multi-gas permeability of column will be dropped dramatically in (Fig. 2). The first stage in the sea, multi-gas merely by 2 pore volume of water, sand column by flooding the permeability coefficient of the former  $4.88 \times 10^{-2} \text{ cm/s}$  to  $1.74 \times 10^{-2} \text{ cm/s}$ , permeability by 64%. As the continuation of displacement, the permeability coefficient some slightly rebounded, but soon stability in the investigation of  $2.15 \times 10^{-2} \text{ cm/s}$  near. The water flooding, only through the process of salt-water about 3 pore volume of solution, and make the permeability coefficient of loss plotted to 56%. To study the reversibility of permeability change, seawater was

used to displace fresh-water to observe the permeability response of sand columns. The results showed that the permeability coefficient only increased from  $2.21 \times 10^{-2} \text{ cm/s}$  to  $2.28 \times 10^{-2} \text{ cm/s}$ , which indicated that the decrease of permeability of sand columns was an irreversible process.

During the second, third and fourth rounds of river water displacement, the permeability of sand samples also decreased significantly, i.e. the permeability coefficient decreased to 38.5%, 28.1% and 20.9% of the initial value, respectively, but the decrease was significantly smaller than that of the first round of river water displacement. The permeability of the sand column decreases slowly during the third- and fourth-wheel displacement. The permeability of sand samples decreased by about 80% in the salinity catastrophe test.

**Fig. 2.** Electrical conductivity of the effluent and the permeability reduction in the experiment

To analyze the reasons for permeability change of sand column, 721 spectrophotometers were used to measure the absorbance of effluent at 600 nm wavelength, and then the standard curve of absorbance and particle concentration was transformed into suspended particle concentration of effluent (Fig. 3). As can be seen from Fig. 3, when the conductivity of the effluent from the sand column reaches 4860, the particles begin to release, but at this time the concentration of particles is very low. After about 25 minutes, the particle concentration reached a maximum of 5, and the effluent was very turbid. After 25 minutes, the particle concentration of the effluent decreases rapidly. The whole process lasts for more than 110 minutes, which is 85 minutes longer than the time to reach the maximum concentration of particles, reflecting the delayed effect of particle release. The whole process of sand column particle release lasted more than 130 minutes, and the cumulative mass of particles released in water-bearing media reached 168 mg.

X-ray diffraction analysis of suspended particles in effluent shows that the released particles include clay minerals and non-clay minerals. Clay particles include illite, kaolinite, chlorite and montmorillonite. Among them, illite accounts for 62% of clay minerals, while kaolinite and montmorillonite account for 13% and 8% of clay minerals respectively, and chlorite only accounts for 3%.

Although clay minerals are rarely found in aquifer samples, they account for 86% of the total released particles. Non-clay minerals mainly include quartz, potassium feldspar and plagioclase, most of which are quartz.

#### 4. Permeability mutations hydro-geochemical mechanism

Through the above experiments, the variation of ion composition in the initial group of displacement process is determined as shown in Fig. 5. It can be seen

from the graph that the concentration of  $\text{Ca}^{2+}$  in effluent varies greatly during the displacement process. The concentration of  $\text{Ca}^{2+}$  in the effluent is much higher than that in local seawater (289.30 mg/L) and underground fresh-water (90.53 mg/L). This is due to the desorption of  $\text{Ca}^{2+}$  in aquiferous media by cation exchange, and the concentration of  $\text{Ca}^{2+}$  in effluent increases and is higher than that in seawater. The change of  $\text{Mg}^{2+}$  concentration is similar to  $\text{Ca}^{2+}$  concentration, but when  $\text{Ca}^{2+}$  concentration reaches the highest value,  $\text{Mg}^{2+}$  has a gentle "step" stage. The reason is that when the exchange of  $\text{Na}^+$ - $\text{Ca}^{2+}$  reaches its limit, the exchanged  $\text{Ca}^{2+}$  does not increase any more. To maintain equilibrium,  $\text{Mg}^{2+}$  begins to join the ranks of cation exchange. The figure shows the "step" stage of  $\text{Mg}^{2+}$  and the "peak" stage of  $\text{Ca}^{2+}$ . Then the equilibrium of solution is broken, the concentration of  $\text{Ca}^{2+}$  in the effluent begins to decrease, and finally  $\text{Ca}^{2+}$ ,  $\text{Na}^+$ ,  $\text{Ca}^{2+}$  and  $\text{Ca}^{2+}$  in the effluent begin to decrease.  $\text{Mg}^{2+}$  tended to be stable.

Because of the rapid change of ion composition, this process must be accompanied by complex hydrologic-geochemical processes. At this time, the clay release sharply and the permeability changes abruptly. Therefore, we use PHREEQC2 software to simulate and calculate the occurrence of calcite and dolomite petrochemical processes. Explain the hydrologic-geochemical processes and their effects on the sudden change of permeability in the mixing process of different proportions of freshwater and sea. Fig.5 shows the saturation index of calcite, dolomite, aragonite and gypsum mixed in different proportions in the displacement process. The line in the Figure is to calculate the saturation index of these four minerals according to the mixing ratio of conservative chloride ions. The saturation indices of calcite, dolomite and gypsum are expressed as follows: calcite saturation index  $SI = [\text{Ca}^{2+}][\text{CO}_3^{2-}]/K$ ; dolomite saturation index  $SI = [\text{Ca}^{2+}][\text{Mg}^{2+}][\text{CO}_3^{2-}]/K$ ; gypsum saturation index  $SI = [\text{Ca}^{2+}][\text{SO}_4^{2-}]/K$ , respectively.

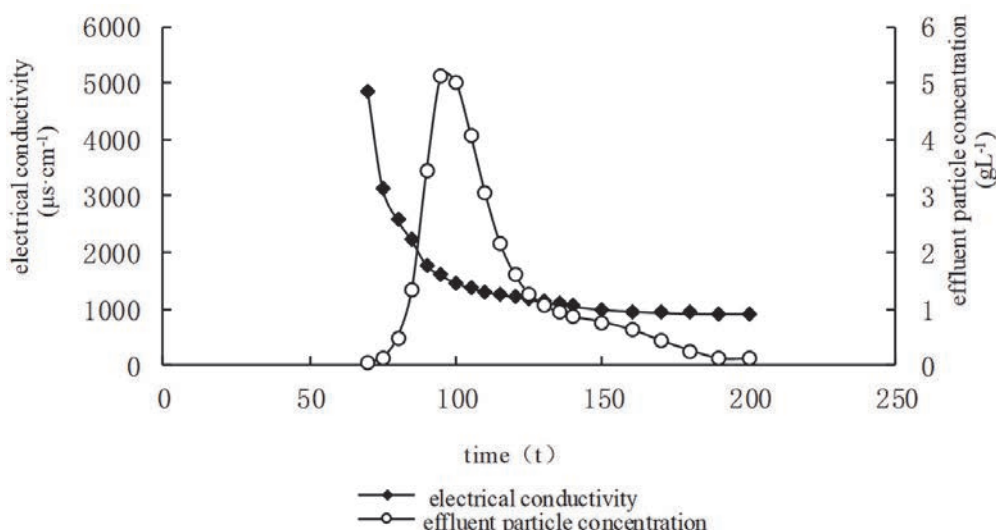
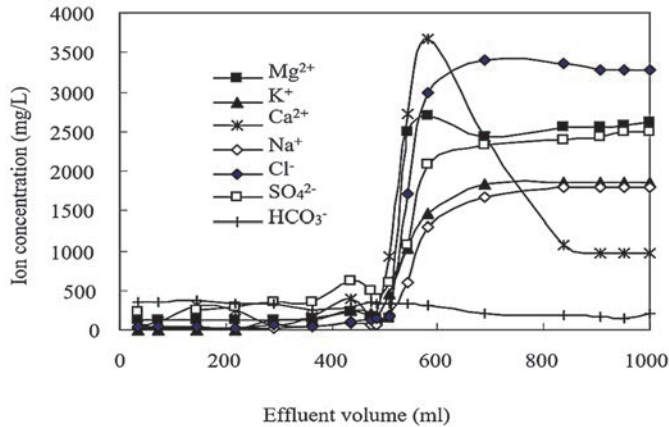


Fig. 3. Particle concentration and electrical conductivity in abrupt salinity experiments



**Fig. 4.** Change curves of ion concentration in the process of seawater displacing freshwater

It can be seen that the variation of saturation index of dolomite, calcite and aragonite is very similar. They all precipitate around 40% of the seawater ratio. At this time, clay release and permeability change abruptly. In Fig.4, the mixing ratio of the sea and fresh-water is about 40%, and the content of  $\text{Ca}^{2+}$  and  $\text{Mg}^{2+}$  reaches the maximum value. It shows that the desorption amount of  $\text{Ca}^{2+}$  and  $\text{Mg}^{2+}$  reaches the maximum when the transgression is 40%, which causes the precipitation of dolomite, calcite and aragonite. The saturation index of gypsum is mostly higher than that calculated by mixing ratio of conservative chloride ions, which indicates that  $\text{SO}_4^{2-}$  has other sources besides seawater. This source is the dissolution of gypsum, which lead the level of  $\text{SO}_4^{2-}$  to

increase. Whether measured or theoretical, the saturation index of gypsum is less than 1, which indicates that gypsum has never reached saturation and the solution is corrosive to gypsum.

Fig.6 shows the dissolution/precipitation of minerals in equilibrium. Among them, the negative value represents the solubility and the positive value represents the precipitation. Dolomite in aqueous solution is unsaturated at the beginning (saturation index  $< 1$ ); when the proportion of seawater to freshwater is 40%, the saturation index reaches 1. Therefore, before the mixing ratio of sea-water to fresh water is 40%, a certain amount of dolomite in aquifer needs to be dissolved to reach the equilibrium state of dolomite in the groundwater mixing solution.

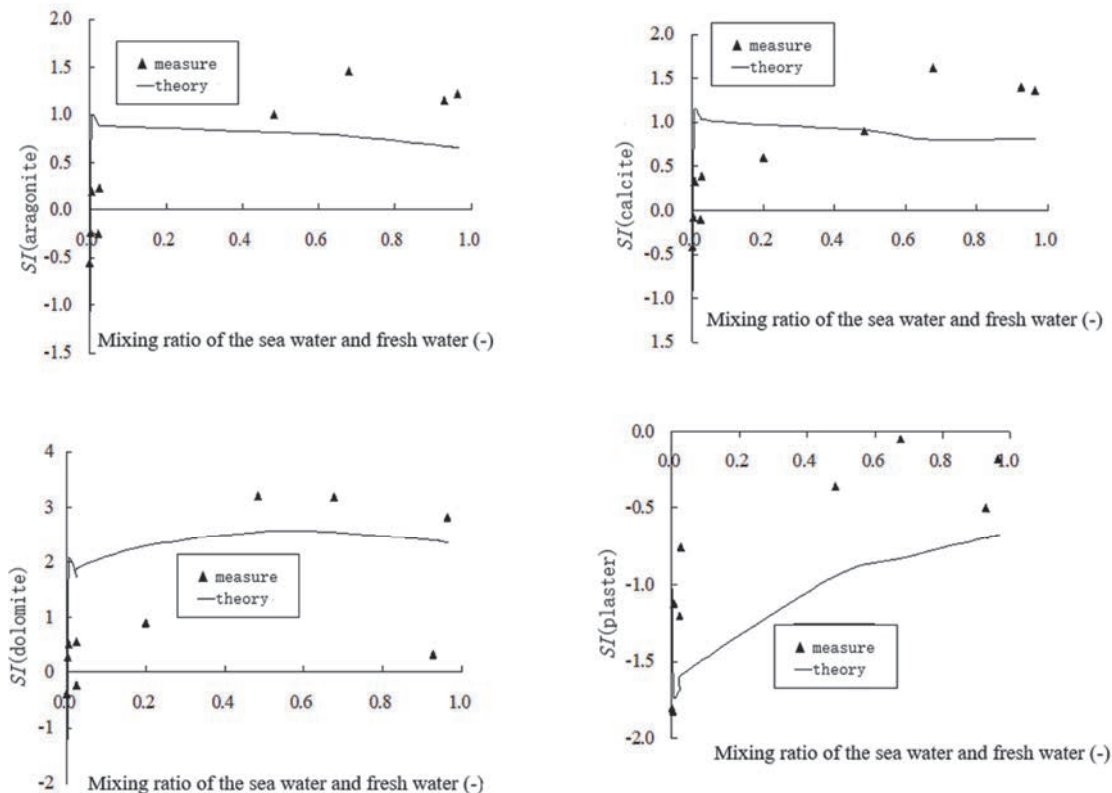


**Fig. 5.** The saturation index of calcite, dolomite, aragonite and gypsum mixed in different proportions in the displacement process

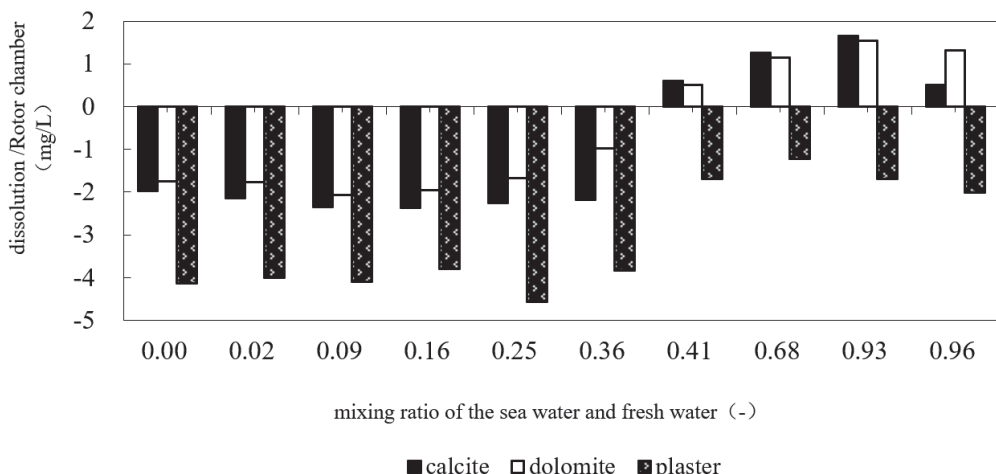


**Fig. 6.** Dissolution/precipitation amounts of minerals during displacement

Dolomite tends to dissolve from the beginning of seawater intrusion to the whole process of 40% intrusion. Then, when the saturation index is greater than 1, the Dolomite Precipitation tends to occur; with the increase of the saturation index, the amount of precipitation increases; when the transgression ratio is 96%, the amount of Dolomite Precipitation decreases. The law of dissolution and precipitation of calcite is similar to that of dolomite. The amount of dissolution/precipitation of the three minerals is very small. Within 5 mg/L, because the soil sample used in the experiment is sandy soil, the content of clay and organic matter is very small, but it is the process of ion exchange and mineral dissolution and precipitation that results in the unbalanced charge of clay minerals in the aquifer medium, resulting in the release of clay particles. The expansion and diffusion of clay particles are enhanced by hydrologic-geochemical action, which results in a decrease of permeability of aquifers.

## 5. Conclusion

(1) The ion exchange action between water and rock exists in the salt-freshwater transition zone,  $\text{Ca}^{2+}$ - $\text{Na}^+$  is the chief part,  $\text{Ca}^{2+}$ - $\text{Mg}^{2+}$  is next,  $\text{Ca}^{2+}$ - $\text{K}^+$  is the least of all. The adsorption capacities of  $\text{Na}^+$ ,  $\text{Mg}^{2+}$  and  $\text{K}^+$  elevate along with the increase of ion concentration in the solution, the desorption of  $\text{Ca}^{2+}$  reaches equilibrium by and large at a high concentration, it is proved that the exchange sites of soil samples are occupied by  $\text{Ca}^{2+}$ .

(2) Infiltration of low salinity water reduces the permeability of different media, even causes blockage, the permeability of sand samples decreased by about 80% in the salinity catastrophe test. The reason for clay release is not the enhancement of diffusion and dispersion, but the enhancement of clay expansion and diffusion by hydro-geochemistry, which results in the decrease of permeability of the aquifer. Thus, cation exchange, mineral dissolution and precipitation, particle release and capture, clay expansion and so on, which can reduce the permeability of aquifers. The cumulative mass of

particles released in water-bearing media reached 168 mg in the experiments.

(3) The proportion of fresh-water to the sea is about 40%. Dolomite, calcite and aragonite begin to precipitate, but the gypsum remains unsaturated and continues to dissolve, the amounts of dissolution/precipitation are relatively small, which are less than 10 mg/L by and large. Because of the ion exchange and mineral dissolution and precipitation process, the charge of clay minerals in the aquifer medium is not balanced, the expansion and diffusion of clay particles are enhanced, and the permeability of aquifer is reduced.

**Acknowledgements.** This article is funded by Shandong Provincial Natural Science Foundation (ZR2017MD009) and National Natural Science Foundation of China (No. 41202165, No. 41102149)

## References

- Appelo C.A.J., Willemsen A., (1987), Geochemical calculations and observations on salt water intrusions, I. A combined geochemical/mixing cell model, *Journal of Hydrology*, **94**, 313-330.
- Beekman H.E., Anthony C., Appelo J., (1990), Ion chromatography of fresh- and salt-water displacement: Laboratory experiments and multicomponent transport modelling, *Journal of Contaminant Hydrology*, **7**, 21-37.
- Chītūm̄ A.D., Moşnegūtū E.F., Nicolescu M.C., Turcu M., Belciu M., Ardeleanu G., (2014), Mathematical modelling of water migration time in soil. *Environmental Engineering and Management Journal*, **13**, 1581-1586.
- Du Q.X., Han Z.Z., Shen X.L., Gao L.H., Han M., (2017), Geochemistry and geochronology of Upper Permian-Upper Triassic volcanic rocks in eastern Jilin Province, NE China: implications for the tectonic evolution of the Palaeo-Asian Ocean, *International Geology Review*, **59**, 368-390.
- Falade A.O., Amigun J.O., Kafisanwo O.O., (2019), Application of electrical resistivity and very low frequency electromagnetic induction methods in groundwater investigation in Ilara-Mokin, Akure

- Southwestern Nigeria, *Environmental and Earth Sciences Research Journal*, **6**, 125-135.
- Han Z.Z., Meng R.R., Yan H.X., Zhao H., Han M., Zhao Y.Y., Sun B., Sun Y.B., Wang J., Zhuang D.X., Li W.J., Li L.X., (2017), Calcium carbonate precipitation by *Synechocystis* sp PCC6803 at different Mg/Ca molar ratios under the laboratory condition, *Carbonates and Evaporites*, **32**, 561-575.
- Kafisanwo O.O., Falade A.O., Bakare O.V., Oresanya A.A., (2018), Reservoir characterization and prospect identification in Onka field, offshore, Niger Delta, *Environmental and Earth Sciences Research Journal*, **5**, 79-86.
- Kong F.M., Liu Y., Li X.P., Guo J.H., Zhao G.C., (2015), Mineralogical and Petrogeochemical characteristics of ultramafic rocks from the metamorphic basement of the Jiaobei terrane, *ACTA Petrologica Sinica*, **31**, 1549-1563.
- Liu Q., Yasufuku N., Miao J.L., Ren J.G., (2014), An approach for quick estimation of maximum height of capillary rise, *Soils and Foundations*, **54**, 1241-1245.
- Mawarni L.W., Maryanto S., Nadhir A., (2018), Magnetic method used in geothermal reservoirs identification in Kasinan-Songgoriti, East Java, Indonesia, *Environmental and Earth Sciences Research Journal*, **5**, 87-93.
- Ochi J., Vernoux J.F., (1998), Permeability decrease in sandstone reservoirs by fluid injection hydrodynamic and chemical effects, *Journal of Hydrology*, **208**, 237-248.
- Ren J.G., Wu Q.Q., Han Z.Z., Gong K., Wang D.S., (2018), Research on the education of industry-education integration for geological majors, *Educational Sciences: Theory & Practice*, **18**, 1315-1322.
- Sen T.K., Khilar K.C., (2006), Review on subsurface colloids and colloid associated contaminant transport in saturated porous media, *Advances in Colloids and Interface Science*, **119**, 71-96.
- Wang D.D., Shi L.Q., (2019), Source identification of mine water inrush: A discussion on the application of hydrochemical method, *Arabian Journal of Geosciences*, **12**, 58.
- Wu Q.Q., Liu G.Q., Zheng X.L., Ren J.G., (2015), Screening of heavy metal tolerant microbes in sludge and their removal capability to lead, *Journal of Residuals Science & Technology*, **12**, 85-91.
- Wu Q.Q., Ren J.G., Han Z.Z., Wang D.S., Gao P.C., Wu Q., (2018), Research on Practice Teaching of Hydrology and Water Resources Specialty, *Educational Sciences: Theory & Practice*, **18**, 2332-2337.
- Xu L.J., Wang G.Y., Liu T.Y., Liu N.Z., Zhang S.C., Zhang T.S., (2018), Optimization of deployment pattern parameters of horizontal well fracturing in tight oil reservoirs, *International Journal of Heat and Technology*, **36**, 1510-1516.
- Yu H., Huang X., Ning J.G., Zhu B.L., Cheng Y., (2014), Effect of cation exchange capacity of soil on stabilized soil strength, *Soils and Foundations*, **54**, 1236-1240.
- Zhang X., Li X.P., Wang Z.L., Zhao L.Q., Shi T.Q., (2016), Mineralogical and petrogeochemical characteristics of the garnet amphibolites in the Xigaze ophiolite, Tibet, *ACTA Petrologica Sinica*, **32**, 3685-3702.